The 2009 IEEE/RSJ International Conference on
Intelligent Robots and Systems
October 11-15, 2009 St. Louis, USA

Surgical Retraction of Non-Uniform Deformable Layers of Tissue: 2D Robot Grasping and Path Planning

Rik Jansen*, Kris Hauser†, Nuttapong Chentanez†, Frank van der Stappen*, Ken Goldberg†

* Department of Information and Computing Sciences, Utrecht University, PO Box 80089, 3508 TB, Utrecht, The Netherlands

† IEOR and EECS Departments, University of California, Berkeley, Berkeley, CA 94720-1777, USA

***Abstract*— This paper considers robotic automation of a common *surgical retraction* primitive of exposing an underlying area by grasping and lifting a thin, 3D, possibly inhomogeneous layer of tissue. We present an algorithm that computes a set of stable and secure grasp-and-retract trajectories for a point-jaw gripper moving along a plane, and runs a 3D finite element (FEM) simulation to certify and assess the quality of each trajectory. To compute secure candidate grasp locations, we use a *continuous spring* model of thin, inhomogeneous deformable objects with linear energy potential. Experiments show that this method produces many of the same grasps as an exhaustive optimization with an FEM mesh, but is orders of magnitude cheaper: our method runs in $O(v \log v)$ time, where v is the number of veins, while the FEM computation takes $O(pn^3)$ time, where n is the number of nodes in the FEM mesh and p is the number of nodes on its perimeter. Furthermore, we present a constant tissue curvature (CTC) retraction trajectory that distributes strain uniformly around the medial axis of the tissue. 3D FEM simulations show that the CTC achieves retractions with lower tissue strain than circular and linear trajectories. Overall, our algorithm computes and certifies a high-quality retraction in about one minute on a PC.**

I. Introduction

Robotic surgical assistants (RSAs) can enhance a surgeon's precision and dexterity in laparoscopic procedures [8], [21], but are currently teleoperated directly as slave devices completely under the surgeon's control. Automation of commonplace surgical tasks could help surgeons focus attention on more critical components of surgery. It may also help surgeons perform complex procedures with three or more manipulators operated simultaneously. Furthermore, automation may enable RSAs to perform procedures in battlefields, where trained medical personnel are scarce, and in remote locations, where large time delays hamper direct teleoperation [22].

This paper describes initial steps toward automating *retraction* in robotic surgery, a common task where an outer covering of tissue is pulled away to expose an area of interest (Fig. 1). We consider a restricted problem, illustrated in Fig. 2. The retraction takes place in 3D, but the 2-point-jaw gripper moves on a 2D plane, and the tissue is assumed to be a thin layer connected at one side. To expose the underlying area of interest with sufficient clearance for subsequent tasks, the gripper must pull the tissue above a line AB (a hard objective). It also should not impart large strains that may damage the tissue (a soft objective). Our problem allows the tissue to be heterogeneous, which we illustrate by embedding stiffer "veins" in the softer surrounding tissue.

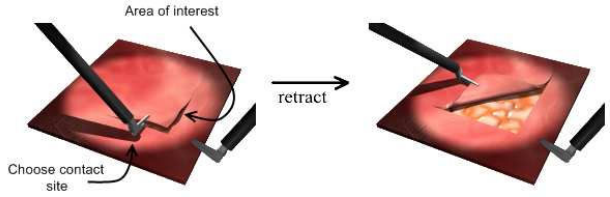

Fig. 1. Automatically retracting a layer of tissue to expose an area of interest. The robot should place its gripper to minimize strain of the retraction.

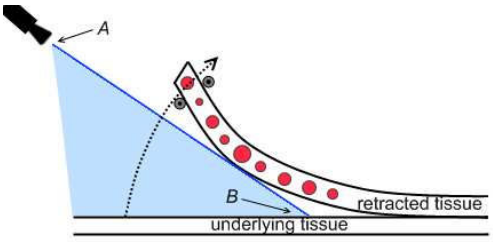

Fig. 2. 2D tissue retraction problem. The RSA must expose a point of interest (point B) to the camera (point A) by moving the tissue to lie completely above AB .

Before executing a retraction on a real patient, we assume that the RSA must be issued a *certificate* from a trusted 3D finite element (FEM) simulator that states the clinical objectives are likely to be achieved (this simulator is assumed given, and outside the scope of this paper). The RSA must find and certify a retraction quickly to remain responsive in the changing surgical environment. We aim to reduce the number of queries to the computationally expensive FEM simulator. To do so, we use simplified models to help generate candidate retractions that are fast to compute, high-quality, and likely (but not guaranteed) to be certified.

These models decompose the 2D cross-section of tissue into orthogonal 1D components. Crosswise, a *continuous spring model* is used to quickly determine a set of candidate grasp locations that make use of tissue heterogeneity to ensure locally *stable* grasp (using a method similar to the D-Space algorithm [7]). Lengthwise, the tissue is treated as a cantilever beam, and we derive an analytical solution for the *constant tissue curvature* (CTC) retraction trajectory for

a given grasp location. Experiments show that the continuous spring model finds many of the same stable and secure grasps that would be computed by the original D-Space algorithm, but is faster by orders of magnitude. We also show the CTC trajectory causes lower tissue strains than circular and linear trajectories. The combined algorithm can typically produce and certify high-quality retraction trajectories in about one minute on a PC.

II. Related Work

A. Robotic surgical assistants

Several robots have been proposed for minimally invasive laparoscopic surgery, for example by Cavusoglu et. al. [4], Guthart and Salisbury [8], and Madhani et. al. [14]. Intuitive Surgical's daVinci^{TM} system has been commercialized and used in thousands of surgical procedures [8]. The surgeon uses a console with visual and tactile feedback to teleoperate a pair of manipulator arms that enter the body cavity. Several methods help improve the precision of such robots, including steady-hand systems [21] and motion scaling [8]. Nevertheless, these procedures remain under direct control of the surgeon. Some semi-supervised robots have been used in specific medical applications, such as neurosurgery [20], radiation therapy [23], and prostate brachytherapy [6].

B. Grasping deformable objects

A large body of work has addressed grasping and fixturing of rigid objects (see Bicchi and Kumar [2] for a survey), with some work extended to deformable objects. Cheong, et. al addressed fixturing problems for an articulated chain of polygons [5]. Cai et. al. and Menassa et. al. investigated deformable sheet-metal parts while minimizing part deformation [3], [16]. Howard and Bekey used a learning approach to enable grasping of deformable objects using tactile feedback [11]. Yu et. al. studied the behavior of controllers for grasping soft tissue [25].

The notion of D-Space was introduced by Gopalakrishnan and Goldberg [7] to characterize the security of grasped deformable parts modeled by a FEM mesh. A configuration in D-Space is represented by all DOFs of the nodes of the mesh, and stable configurations require positive work to release the object from its grasp. An algorithm for finding an optimal jaw separation distance was also introduced for a two-point gripper that balances the energy needed to release the part against the energy needed to compress it into plastic deformation [7]. We use a simplified version of this technique to select secure grasps of a thin tissue layer.

C. Manipulating deformable objects

A number of researchers have addressed motion planning for deformable linear objects such as ropes and cables. Saha et. al. describe a sampling-based motion planner for rope manipulation with two cooperating robot arms [19]. Moll and Kavraki describe a method for computing energy-minimizing curves subject to manipulation constraints, and apply them to surgical suturing problems [17]. Holleman et. al. and Lamiraux and Kavraki developed path planners for elastic surface patches [10], [13]. The surface patch is modeled as a Bezier surface with low bending energy, and a sampling-based planner is used to plan the path.

Other work has addressed planning for volumetric deformations. Rodriguez et. al. applied sample-based planning to deformable objects in deformable 3D environments [18]. Alterovitz et. al. used a numerical optimization approach to plan needle paths in 2D deformable tissue for prostate brachytherapy [1]. Hirai et. al. [9] presented the use of visual feedback to position points in 2D deformable tissue, which was applied in breast biopsies [15] and prostate brachytherapy [24].

III. Problem Statement

A. Tissue and Robot Modeling

We model the tissue as a 3D elastic deformable body E, which we assume is a thin layer of uniform thickness having known material properties. For simulation purposes, E is represented into a tetrahedral FEM mesh. Heterogeneous tissue is modeled by a mesh with varying stiffness. The D-Space of all 3D FEM mesh configurations is denoted by D, and $q \in D$ describes all positions of the simulation nodes. We forward simulate FEM dynamics using the method of Irving et. al. [12]. Our retraction algorithms assume that the tissue is damped and velocities of the jaws remain low, such that the tissue moves smoothly between time steps and its motion can be approximated as a quasi-static process.

The gripper is modeled by two point contacts moving on a planar cross section of 3D space. We take a frame of reference such that the bottom edge of the tissue cross section lies on the x axis, and gravity acts in the $-y$ direction. The 4D space of robot configurations is denoted C.

B. Retraction Trajectories

A retraction is a robot trajectory $c(t) : [0, T] \mapsto C$, for some unknown termination time T. We do not consider how the robot moves before it makes initial contact, so that the jaws are instantaneously placed at points on the perimeter of the tissue at time $t = 0$. First, the jaws are compressed, and then the gripper is moved while keeping the distance between jaws fixed. At time $t > 0$, the motion of the tissue in response to $c(t)$ can be computed by evaluating the FEM simulation. Let this path be denoted $q_c(t) : [0, T] \mapsto D$.

C. Visibility, Grasp Security, and Strain Objectives

Our problem is to produce a retraction $c(t)$ and a termination time T that meets the following objectives.

1) *Visibility*. Given view point A and a point B on the area of interest, we require that at time T the tissue at configuration $q_c(T)$ lies above line AB.
2) *Grasp security*. Grasp points must stay fixed relative to the tissue throughout the retraction (i.e. do not break contact or slip). We assume the friction coefficient μ between the gripper and tissue is known.
3) *Admissible strain*. To cope with noise and discretization artifacts in the FEM mesh, we require that the

average strain $\epsilon_{max}(c)$ of the 1% volume elements with the highest strain does not exceed the strain limit ϵ_L.

The FEM simulation issues a certificate to retraction $c(t)$ if these objectives are satisfied after $c(t)$ is simulated. We assume that the simulation is trusted by the surgeon, so that a certified retraction is safe to execute on the patient. We consider strain as a soft objective function, so given multiple certified trajectories we select the retraction with lowest $\epsilon_{max}(c)$.

IV. Method

Our approach generates a number of candidate retractions (up to a user-defined maximum), and tests the objectives of Section III-C by evaluating the FEM simulation. To generate the retractions, we first pick a set of contact pairs p_a and p_b which are likely to be locally stable, using a simplified linear spring model. For each contact pair p_a and p_b, we first close the jaws to a distance that trades off stability against tissue strain. Then, holding the distance constant, we move the gripper along a trajectory that is optimal if the tissue layer is viewed as a homogeneous cantilever beam under no gravity.

A. Choosing stable grasp locations

We choose grasp locations that are locally optimal with respect to the grasp security and admissible strain objectives, while we consider the visibility constraint at a later stage. Gopalakrishnan and Goldberg [7] define *stable* grasps as pairs of perimeter nodes that are located at local minima in the elastic potential of the FEM mesh, and they describe an algorithm that finds a jaw distance that trades off stability against plastic deformation. Finding the optimal distance for a n-nodes mesh with p perimeter nodes takes $O(n^3p^2 + p^6 \log p)$ time. Our approach uses the same concepts, but introduces simplifications appropriate for a thin rectangular mesh.

1) Stable grasps and escape energy: We require that the jaws must be directly opposite the mesh surface, as illustrated in Fig. 3, which reduces our problem to finding a horizontal translation x along the length of the tissue. Consider tissue stiffness as a function of x. We let $k_{eq}(x)$ denote the *equivalent spring constant*, which represents the amount of force at x needed to compress the tissue a unit distance. We characterize the stability of a grasp location x by its ability to resist shifting to a neighboring spring. That is, a grasp at x is *stable* if positive work is needed to shift the grasp from x to x'. This is precisely the case where x corresponds to a local minimum of $k_{eq}(x)$.

Escaping the basin of attraction of a stable grasp requires sliding the grasp past a local maximum of $k_{eq}(x)$. We use the following *escape potential* metric to characterize the stability of a stable grasp location x:

$$Escape(x) = \min(k_{eq}(x_r), k_{eq}(x_l)) - k_{eq}(x)$$

where x_r and x_l are respectively the local maxima to the right and left of x. Thus, to find all stable grasp locations and calculate their escape potential, we must simply find the extreme points of k_{eq}.

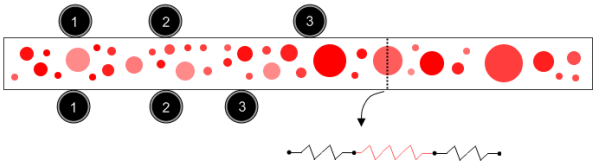

Fig. 3. A continuous model for representing heterogeneous tissue. Darker shaded areas represent veins. Jaws as shown in positions 1 and 2 are allowed. Asymmetric grasps, such as position 3, are not allowed. The line segment running from the upper surface to the lower surface between the jaws is considered as a serial connected spring with varying spring constants.

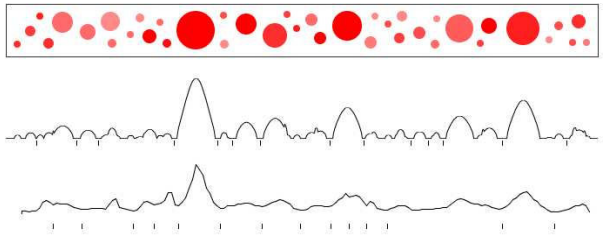

Fig. 4. Top: tissue model. Middle and bottom: equivalent spring constants and stable grasp locations obtained by the continuous spring method (middle) and brute-force FEM simulations (bottom).

2) Locally stable grasp locations using a continuous spring model: Though, in principle, it would be possible to compute k_{eq} using the FEM model, we use a much faster *continuous spring model* approximation. This model approximates the tissue's compression behavior as a vertical linear spring along a slice through the tissue (Fig. 3). This approximation decouples each slice from its neighboring tissue, and therefore ignores interactions due to shear stress. If the tissue is sufficiently thin, shear stresses will not affect the compression behavior much.

Consider the line segment $s_{cross}(x)$ running vertically through the tissue between the jaws placed at x. We can decompose it into multiple line segments s_i with length $l_i(x)$, each of which has constant Young's moduli E_i and infintesimal cross section A. Each segment s_i can be considered as a spring with spring constant $k_i(x) = \frac{E_i}{l_i(x)}$. The combined serial spring $s_{cross}(x)$ has an equivalent spring constant $k_{eq}(x)$:

$$k_{eq}(x) = \frac{1}{\sum_{i=1}^{n} \frac{1}{k_i(x)}} = \frac{1}{\sum_{i=1}^{n} \frac{l_i(x)}{E_i}}. \quad (1)$$

If veins are represented as polygons with v vertices, we can compute the extreme points of k_{eq} using a sweep line algorithm. We note that the extreme points of $k_{eq}(x)$ are also extreme points of $\frac{1}{k_{eq}(x)}$, and $\frac{1}{k_{eq}(x)}$ is a sum of linear functions. Considering vertices as event points, we find when $1/k_{eq}(x)$ changes slope for each vertex encountered in the event queue. Sorting the queue takes $O(v \log v)$ time, and each of the v event points can be evaluated in $O(1)$ time, which leads to an $O(v \log v)$ running time overall.

Fig. 4 shows an example of the equivalent spring constant function constructed by the sweep-line method using a fine polygonalization of the veins.

B. Choosing an optimal jaw distance

Once we have chosen a location to grasp the tissue, we must choose a compression distance σ. We use a criterion similar to the one used in Gopalakrishnan and Goldberg [7] that balances the competing objectives of grasp security and low strain, in particular, we choose σ such that the energy needed to release the grasp is equal to the energy needed to exceed the strain limit. Consequently, jaw compression can be reduced when the tissue is heterogeneous and the grasp location is locally secure (i.e., bordered by relatively stiff veins). In turn, this reduces tissue strain.

We choose σ as follows. Let the tissue at the grasp point have the equivalent spring constant k_{eq}. Closing the jaws to distance σ induces strain $\epsilon = 1 - \sigma/L$ where L is the rest height of the tissue. The elastic strain limit ϵ_L imposes the constraint $\sigma \geq (1 - \epsilon_L)L$. Given σ, the amount of energy needed to compress the spring to the strain limit is

$$U_L(\sigma) = \frac{1}{2} k_{eq} (\sigma - (1 - \epsilon_L)L)^2 \tag{2}$$

We also find the two locally stiffest parts of the tissue that neighbor the grasp point. Pick the least stiff of the two, and let k_n denote its equivalent spring constant. If the tissue is locally homogeneous, we set $k_n = k_{eq}$. The amount of energy U_n to compress the neighboring spring a distance σ equals:

$$U_n(\sigma) = \frac{1}{2} k_n \sigma^2 \tag{3}$$

We choose σ such that (2) and (3) are equal:

$$\sigma = \frac{\sqrt{k_{eq}}(1 - \epsilon_L)L}{\sqrt{k_{eq}} + \sqrt{k_n}} \tag{4}$$

C. Choosing a Retraction Trajectory

After finding grasp locations p_a, p_b and a jaw separation distance σ, we must find a path of the manipulator to retract the tissue. Some simple paths (e.g. straight lines and circular arcs) can achieve the retraction objectives without causing excessively high strains, because the largest strains are usually caused by the squeezing of the gripper. But, they do stretch the tissue unnecessarily. Therefore, we introduce a *constant tissue curvature* (CTC) trajectory that keeps the medial axis of the tissue stretch-free and bend with a constant curvature. This trajectory produces minimal strain if the tissue is treated as a weightless homogeneous cantilever beam that can bend and stretch, where stretching strain is much higher than bending strain. This latter assumption implies that the length of the tissue should be kept constant. With length held constant, theories on beams prescribe that curvature should be uniform to minimize the maximum bending strain.

Place a coordinate frame with its origin at the lower-right corner of the tissue. Let $-L$ denote the position of the grasp point. Along $c(t)$, the lower edge of the tissue must describe a circular arc with constant length L but time-varying radius $R(t)$ and center $(0, R(t))$, as illustrated in Fig. 5. At $t = 0$, we have $R(t) = \infty$ and as t increases, $R(t)$ decreases, moving the center of the circle along the y-axis toward the x-axis. At the end time $t = T$, the arc must lie to the right of the line-of-sight.

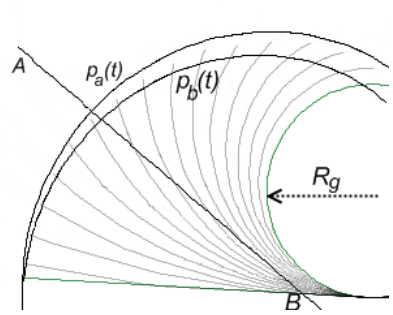

Fig. 5. The trajectories $p_a(t)$ and $p_b(t)$ the jaw nodes follow during the retraction. The CTC path keeps the medial axis of the tissue circular with radius $R(t)$, length x, and, in the final configuration, lies tangent to the line-of-sight AB.

We compute the goal radius $R_g = R(T)$ to be tangent to the line-of-sight. With a bit of algebra, this can be shown to be:

$$R_g = \frac{|A - B||b_x a_y - a_x b_y| - (a_x - b_x)(a_x b_y - b_x a_y)}{(a_y - b_y)^2} \tag{5}$$

where $A = (a_x, a_y)$ and $B = (b_x, b_y)$. Intermediate tissue radii $R(t)$ are linearly interpolated in curvature as $R(t) = R_g \frac{T}{t}$.

At the tissue configuration at time t, the medial axis of the tissue will coincide with an arc of the circle with center $(0, R(t))$, but with radius $R(t) - \frac{1}{2}h$. Sliding along this arc with arclength L, we compute the point $p(t)$:

$$\begin{aligned} p(t) &= ((R(t) - \tfrac{1}{2}h)\cos\theta, (R(t) - \tfrac{1}{2}h)\sin\theta + R(t)) \\ \theta(t) &= \tfrac{L}{R(t) - \frac{1}{2}h} + \tfrac{3}{2}\pi \end{aligned}$$

where the angle of the gripper θ is chosen to keep the arclength fixed. At $c(t)$, the projections of the jaw locations on the medial axis should coincide with $p(t)$. Incorporating the jaw separations σ, the final CTC trajectory is:

$$\begin{aligned} p_a(t) &= (R_a(t)\cos\theta(t), R_a(t)\sin\theta(t) + R_a(t)) \\ p_b(t) &= (R_b(t)\cos\theta(t), R_b(t)\sin\theta(t) + R_a(t)) \\ R_a(t) &= R(t) - \sigma \\ R_b(t) &= R(t) + \sigma - h \end{aligned}$$

where p_a and p_b denote the location of the lower and upper jaw respectively. An illustration of such a path is given in Fig. 5.

To ensure the tissue is pulled past the line-of-sight in the presence of gravity and inhomogeneity, we generate a retraction trajectory that goes much longer than T, and let the FEM simulation run only until all objectives are met, or some constraint is violated.

V. Experiments

All results in this section were obtained on a tissue model having dimension of 5.0 cm in length and 0.44 cm in height and depth, and density of 1 g/cm^3. For 3D simulation we use Young Modulus and Poisson Ratio of 40 kPa and 0.45 respectively for the tissue and 200 kPa and 0.45 respectively

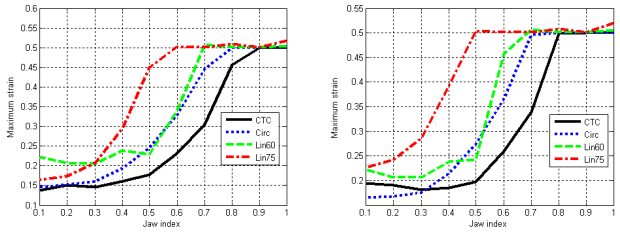

(a) (b)

Fig. 6. Comparing linear, circular and the CTC trajectories for two lines-of-sight, starting at distance (a) 25% and (b) 15% from the fixed end of the tissue. Each line-of-sight has 45° slope. Strain of 0.5 means failure.

for the vein. We set $\epsilon_L = 0.5$, and $\mu = 0.5$ throughout all experiments. The gravity for the dynamic simulation is set to 9.8 m/s^2 downward. All experiments were performed on a PC with a 1.8 GHz processor and 2 GB of RAM.

A. Assessment of Grasp Selection Quality

We compare our continuous spring method of finding locally stable grasp locations to brute-force simulations with the commercial FEM package ANSYS. The FEM mesh contains 10,000 nodes and 160 pairs of opposite perimeter nodes. In ANSYS, we enumerated each pair of opposite perimeter nodes, contracted a unit distance and solved for the maximum strain in the tissue. The ANSYS simulation took 16 minutes and 32 seconds, while the spring method took 0.1 seconds. Fig. 4 shows the equivalent spring constant function k_{eq}, and indicates the top 15 grasp locations as computed by brute-force simulation and by our spring model. The spring model finds 8 out of 15 stable and secure grasp locations as computed by ANSYS.

B. Assessment of Retraction Path Strains

In the following experiments, we use our 3D FEM simulator to compare the quality of our retraction trajectories (as described in Sec. IV-C) against linear and circular paths, which are attractive for their relative simplicity. For varying grasp location, we run linear paths with (1) 60° and (2) 75° slopes, (3) a circular path and (4) the CTC trajectory. In the linear and circular paths, we adjust the jaw orientations such that they are perpendicular to the line from the fixed end to the jaw's midpoint.

1) Experiments on homogeneous tissue: Fig. 6 plots the maximum strain during the simulation on homogeneous tissue with gravity for two lines-of-sight for 10 uniformly sampled grasping locations. We can see that the CTC path performs better than the circular and linear paths in all cases, even for suboptimal grasp locations.

Repeating the same experiment for other lines-of-sight, we found that the CTC trajectory almost always outperforms the other paths, except when the line-of-sight lies close to the fixed end of the tissue (approximately 25% away from the fixed end). In these cases, circular trajectories perform slightly better for certain grasp locations near the free end of the tissue.

In another set of experiments in homogeneous tissue we found that the optimal jaw location is relatively insensitive

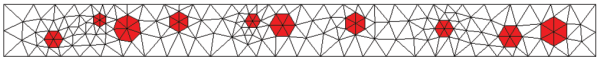

Fig. 7. Side view of 3D FEM mesh containing 10 veins.

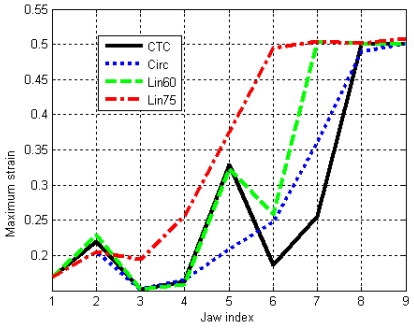

Fig. 8. Comparing linear, circular, and constant-tissue-curvature (CTC) paths for heterogeneous tissue containing 10 veins. An index of i means the jaw is in a stable location between the i-th and $(i+1)$-th vein.

to problem parameters (e.g., line-of-sight, tissue thickness, and friction), and nearly always lies between 10% and 20% from the free end of the tissue.

2) Experiments on heterogeneous tissue: In this section, we consider a heterogeneous tissue containing 10 veins (Fig. 7). For all candidate grasp locations found by the continuous spring method, we ran the 3D simulation using the linear, circular and CTC paths. Results are shown in Fig. 8. Both the CTC and the circular path are able to find the optimal jaw location between veins 3 and 4.

For suboptimal jaw locations, the CTC path usually outperforms other paths, except the circular path performs substantially better at jaw location 5. (Even under further scrutiny, we are unable to discern a clear cause for this behavior.) Apart from these occasional anomalies, this and other experiments suggests that the CTC trajectory still works well with heterogeneous tissue, even if a homogeneity assumption was used in its derivation.

C. Efficient Certification of Multiple Retractions

Given the multiple retractions computed by the continuous spring model, we wish to certify and choose the retraction that minimizes the maximum strain $\epsilon_{max}(c)$. Rather than run the FEM simulation in full for each retraction, we terminate simulations immediately when the hard objectives of Sec. III-C fail, or $\epsilon_{max}(c)$ exceeds the maximum strain computed for any prior certified retraction (because then c is suboptimal).

Our experiments in the heterogeneous tissue of Fig. 7 suggest that this pruning technique reduces running time from 286s to 76s for 10 veins. On a more complex mesh with 20 veins, pruning reduces running time from 819s to 95s. In most cases, the simulation trials were pruned early on, as strain is accumulated quickly during the compression phase and at the beginning of retraction.

D. Optimal Retraction for a Wide Piece of Tissue

Fig. 9 shows a screenshot from a retraction computed by our algorithm on a 3.5 cm wide heterogeneous tissue. The full

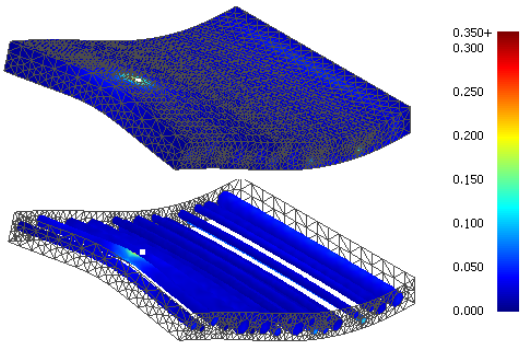

Fig. 9. A frame from a 3D simulation of a 5 cm x 3.5 cm x 0.44 cm heterogeneous mesh with 20 veins, showing the surface of the mesh (top) and the veins (bottom). Strain is color coded.

animation accompanies this paper as a supplemental video.

VI. Conclusion and Future Work

This paper introduced a method to compute a trajectory for a two-point gripper, moving in a plane, to retract a thin layer of tissue under visibility and tissue strain constraints. We present a continuous spring model for finding locally stable candidate grasps in $O(v \log v)$ time, where v is the number of veins embedded in the tissue. For each candidate grasp location, we compute a retraction trajectory that causes a cantilever beam model of the tissue to follow a constant curvature arc. These retractions are then certified using a 3D finite element simulator. Experiments suggest that 1) the continuous spring approximation quickly computes many of the same grasp locations as an expensive FEM-based computation, and 2) constant-tissue-curvature paths produce lower tissue strains than circular or linear paths. Our algorithm can certify and select a high-quality retraction in about one minute on a PC.

In future work we hope to address more realistic manipulator models with geometric and kinematic constraints and obstacles. In such a setting, regrasping may be necessary because of the limited accessibility of grasp points and limited range of motion of the tissue. More realistic tissue damage models would measure cellular damage as a function of strain and duration of applied load. Our method also does not perform the sophisticated spatial reasoning needed to find optimal retractions of thick tissue and retractions where tissue must be pulled apart rather than lifted. Similar reasoning would be necessary to optimize incision patterns and retractions simultaneously.

Acknowledgments

This work was partially supported under NIH Research Award R01EB-006435-01A1. We thank M. C. Cavusoglu, W. Newman, and P. Abbeel for inspiring discussions. We would also like to thank R. Alterovitz and V. Duindam for thoughts and advice, and S. Faridani for help on ANSYS.

References

[1] R. Alterovitz, K. Goldberg, J. Pouliot, R. Taschereau, and I.-C. Hsu. Sensorless planning for medical needle insertion procedures. In *IEEE/RSJ Int. Conf. Int. Rob. and Sys.*, pages 3337–3343, Oct.

[2] A. Bicchi and V. Kumar. Robotic grasping and contact: a review. In *IEEE/RSJ Int. Conf. Int. Rob. and Sys.*, pages 348–353, 2000.

[3] W. Cai, S. J. Hu, and J. X. Yuan. Deformable sheet metal fixturing : Principles, algorithms, and simulations. *J. of Manufacturing Science and Engineering*, 118(3):318–324, 1996.

[4] M. Cavusoglu, F. Tendick, M. Cohn, and S. Sastry. A laparoscopic telesurgical workstation. *IEEE Trans. Rob. and Aut.*, 15(4):728–739, Aug 1999.

[5] J.-S. Cheong, K. Goldberg, M. Overmars, and A. van der Stappen. Fixturing hinged polygons. In *IEEE Int. Conf. Rob. and Aut.*, pages 876–881, 2002.

[6] G. Fichtinger, E. C. Burdette, A. Tanacs, A. Patriciu, D. Mazilu, L. L. Whitcomb, and D. Stoianovici. Robotically assisted prostate brachytherapy with transrectal ultrasound guidance–phantom experiments. *Brachytherapy*, 5(1):14–26, Jan. 2006.

[7] K. G. Gopalakrishnan and K. Goldberg. D-space and deform closure grasps of deformable parts. *Int. J. of Rob. Res.*, 24(11):899–910, 2005.

[8] G. Guthart and J. Salisbury, J.K. The intuitive^{TM} telesurgery system: overview and application. In *IEEE Int. Conf. Rob. and Aut.*, pages 618–621 vol.1, 2000.

[9] S. Hirai, T. Tsuboi, and T. Wada. Robust grasping manipulation of deformable objects. In *IEEE Int. Symp. Assembly and Task Planning*, May 2001.

[10] C. Holleman, L. Kavraki, and J. Warren. Planning paths for a flexible surface patch. In *IEEE Int. Conf. Rob. and Aut.*, volume 1, pages 21–26, May 1998.

[11] A. M. Howard and G. A. Bekey. Recursive learning for deformable object manipulation. In *Proceedings of the 8th Int. Conf. on Advanced Robotics*, pages 939–944, 1997.

[12] G. Irving, J. Teran, and R. Fedkiw. Invertible finite elements for robust simulation of large deformation. In *Symp. on Computer Animation*, pages 131–140, 2004.

[13] F. Lamiraux and L. E. Kavraki. Path planning for elastic plates under manipulation constraints. In *IEEE Int. Conf. Rob. and Aut.*, pages 151–156, 1999.

[14] A. Madhani, G. Niemeyer, and J. Salisbury, J.K. In *IEEE/RSJ Int. Conf. Int. Rob. and Sys.*

[15] V. Mallapragada, N. Sarkar, and T. Podder. Robot assisted real-time tumor manipulation for breast biopsy. In *IEEE Int. Conf. Rob. and Aut.*, 2008.

[16] R. Menassa and W. D. Vries. Optimization methods applied to selecting support positions in fixture design. *ASME J. of Engineering for Industry*, 113:412–418, 1991.

[17] M. Moll and L. Kavraki. Path planning for deformable linear objects. *IEEE Trans. Robotics*, 22(4):625–636, Aug. 2006.

[18] S. Rodriguez, J.-M. Lien, and N. M. Amato. Planning motion in completely deformable environments. In *IEEE Int. Conf. on Robotics and Automation*, pages 2466–2471, Orlando, FL, May 2006.

[19] M. Saha and P. Isto. Motion planning for robotic manipulation of deformable linear objects. In *IEEE Int. Conf. Rob. and Aut.*, pages 2478–2484, May 2006.

[20] G. Sutherland, P. McBeth, and D. Louw. Neuroarm: An mr compatible robot for microsurgery. In *Computer Assisted Radiology and Surgery*, volume 1256, pages 504–508, 2003.

[21] R. Taylor, P. Jensen, L. Whitcomb, A. Barnes, R. Kumar, D. Stoianovici, P. Gupta, Z. Wang, E. Dejuan, and L. Kavoussi. A Steady-Hand Robotic System for Microsurgical Augmentation. *Int. J. of Rob. Res.*, 18(12):1201–1210, 1999.

[22] R. H. Taylor. Robots as surgical assistants: Where we are, wither we are tending, and how to get there. In *AIME '97: Proceedings of the 6th Conf. on Artificial Intelligence in Medicine in Europe*, pages 3–11, London, UK, 1997. Springer-Verlag.

[23] R. Z. Tombropoulos, J. R. Adler, and J. Latombe. Carabeamer: A treatment planner for a robotic radiosurgical system with general kinematics. *Medical Image Analysis*, 3:3–3, 1999.

[24] M. Torabi, K. Hauser, R. Alterovitz, V. Duindam, and K. Goldberg. Guiding needle insertions using single-point tissue manipulation. In *IEEE Int. Conf. Rob. and Aut.*, May 2009.

[25] X. Yu, H. J. Chizeck, and B. Hannaford. Comparison of transient performance in the control of soft tissue grasping. In *IEEE/RSJ Int. Conf. Int. Rob. and Sys.*, San Diego, CA, October 2007.